Journal of
Mechanics of
Materials and Structures

GEOMETRICALLY NONLINEAR THERMOMECHANICAL RESPONSE OF
CIRCULAR SANDWICH PLATES WITH A COMPLIANT CORE

Yeoshua Frostig and Ole Thomsen

GEOMETRICALLY NONLINEAR THERMOMECHANICAL RESPONSE OF CIRCULAR SANDWICH PLATES WITH A COMPLIANT CORE

YEOSHUA FROSTIG AND OLE THOMSEN

The geometrically nonlinear response of a circular sandwich plate that consists of two face sheets and a compliant ("soft") core with mechanical properties that may be either independent or dependent of temperature and subjected to both mechanical loads and thermal induced deformations, but remain elastic linear throughout the loading process, is presented. The mathematical formulation follows the principles of the high-order sandwich panel theory (HSAPT) and includes the vertical flexibility of the core in addition to the temperature dependency of the mechanical properties of the core material. The mathematical formulation outlines the set of governing partial differential equations as well the appropriate boundary conditions for a general sandwich layout. The particular case of an axisymmetric circular sandwich plate subjected to axisymmetric mechanical and thermal loads, and with axisymmetric boundary conditions is studied analytically and numerically. The numerical study includes an interaction of mechanical and thermal loads which is presented through results within the plate for various load levels of various structural quantities as well as equilibrium curves of temperatures versus these structural quantities. The results reveal that the combination of mechanical and thermal loads along with a compliant core material with mechanical properties that degrade with increasing temperatures shifts the behavior from a linear and stable (strength controlled) response into a strongly nonlinear response with limit point behavior and associated loss of stability, when large displacements and large rotations (geometrical nonlinearity) are included in the modeling.

1. Introduction

Lightweight sandwich structures are being used increasingly in the aerospace, naval and transportation industries due to their excellent stiffness-to-weight and strength-to-weight ratios. Typical sandwich structures are often composed of a low stiffness/strength (compliant or "soft") core material made of a polymeric foam or a Nomex® honeycomb that is flexible in the thickness direction, and laminated composite or metallic face sheets. The core usually provides the shear resistance/stiffness to the sandwich structure, as well as vertical (through-thickness) support to the face sheets that is associated with core vertical normal stresses. The use of compliant foam or Nomex core materials is often associated with localized effects such as indentation in case of localized, concentrated or line loads, abrupt geometrical changes or changes of mechanical properties as well as in the vicinity of stiff points such as inserts or supports. Thus, the low core through-thickness stiffness may be detrimental to the safety of a sandwich structure, either because of strength constraints such as stress allowables or due to loss of stability.

Sandwich structures are typically exposed to mechanical load as well as to aggressive environment

that may be associated with elevated temperature conditions. Traditionally, a typical design process of such structures examines separately the responses due to the mechanical and thermal loads, i.e., the deformations induced by thermal sources. However, the interaction between the mechanical and thermal loads may lead to an unsafe response with loss of stability and structural integrity, especially when the deformations are large and the mechanical properties such as stiffness and strength degrade as the temperature level is raised. This thermal degradation of the mechanical properties is especially pronounced for polymer foam core materials, where significant degradation of the mechanical properties may occur well within the operational temperature range. For example, PVC foams such as Divinycell® (see [DIAB 2003]) lose all stiffness and strength at about 80–100°C, while PMI (polymethacrylimide) foams such as Rohacell® (see [Rohacell 2004]) lose heat distortion resistance at about 200°C.

The effects of this degradation on the load-thermal interaction response are not well understood by researchers and industry. At the same time there is growing concern within the wind turbine blade, marine and aeronautical sectors that the simultaneous action of mechanical loads and elevated temperatures may compromise the structural integrity under certain circumstances. Hence, reliable computational models are needed for the accurate prediction of the load response of sandwich structures subjected to combine mechanical and thermal loads, including the thermal degradation of material properties as well as the nonlinear interactions between the mechanical and thermal loads. In the present paper such a model based on the principles of the high-order sandwich panel theory (HSAPT) is proposed for the case of circular sandwich plates.

Generally, two main categories are presented in the literature to describe the load response of sandwich structures. The first category assumes the sandwich structures to be compressible in the through-thickness direction, and the other category of models is based on the assumption of through-thickness incompressibility, i.e., infinite stiffness in the through-thickness direction, which is also known as antiplane core conditions; see [Allen 1969]. The majority of structural models assume that the core is incompressible; see for example the textbooks and review articles [Allen 1969; Plantema 1966; Zenkert 1995; Vinson 1999; Noor et al. 1996; Librescu and Hause 2000; Hohe and Librescu 2004]. However, in reality a sandwich structure is a layered structure with two face sheets and a core that compressible (has finite stiffness). The effect of the through-thickness core compressibility has been considered in through the use of the HSAPT models, and by others as well; see for example [Petras and Sutcliffe 2000]. A large number of computational models have been proposed based on the assumption of incompressible sandwich panels, and in most of these the layered sandwich assembly is replaced with an equivalent single layer (ESL); see for example [Mindlin 1951; Reddy 1984].

The same two categories of models — with compressible or incompressible core — have been proposed for circular sandwich plates. Computational models for sandwich plates with an incompressible core using the ESL approach have been considered for both static and dynamic applications by many researchers, including Selke [1971], who used the Reissner approach to analyze a mirror made of an annular sandwich plate resting on a ring; Montrey [1973], who used the split rigidities approach of [Allen 1969] to investigate the linear static response of a load introduced through an insert to a circular sandwich plate; Gupta and Sharma [1982], who used the zigzag approach of [Allen 1969]; and Wang [1995a; 1995b], who used Reissner–Mindlin first-order shear deformable theory for the analysis of radially symmetric circular plates. In all the references mentioned the core is assumed to be incompressible, and in most cases the problem considered is radially symmetric. Thermal effects have been considered by Kao [1970]

assuming that the core is incompressible, the face sheets are membranes, and the through-thickness shear is being carried by the core only.

Vibration analyses of circular sandwich plates been considered by many researchers, including Gupta and Jain [1982], who used first-order shear deformable plate theory (FOSDPT) to determine the dynamic response of a circular sandwich plate with a variable thickness assuming polynomial type of modes; Sherif [1992], who used a similar approach for the nonlinear dynamic problem where the core is viscoelastic and the modes are of polynomial type; and Du [1994] and Du and Li [2000] who discussed the radially symmetric large amplitude free vibration of circular sandwich plates assuming that the face sheets are membranes. Notice that the quoted models are limited to axisymmetric or isotropic plate behavior, to membrane action with no bending effects in the face sheets, and to incompressible cores. Zhou and Stronge [2006] used the FOSDPT approach assuming some special modes to deal with the vibration of a circular sandwich plate of a general layout.

The effect of the out of plane flexibility of the compressible core for circular plates has been considered in [Thomsen 1995; 1997; Thomsen and Rits 1998] using an elastic foundation and the HSAPT approaches, respectively. Rabinovitch and Frostig [2002a] used the HSAPT approach to investigate the response of a circular sandwich plates that are either fully bonded or debonded, and they used a similar approach to study the response of an reinforced concrete (RC) circular plate strengthened with a circular patch with an axisymmetric layup [2002b], with a general non-axisymmetric layout [2004a], and a with a delaminated patch [2004b]. In all these cases the computational models are limited to linear, small deformations. Recently, Santiuste et al. [2011] investigated the thermal-mechanical response of circular sandwich plates including thermal degradation of the core properties, large displacements and rotations and assuming axially symmetric loads and boundary condition. The paper emphasizes on the nonlinear finite element analysis of such structures with some comparison with the axisymmetric HSAPT model results.

The literature survey reveals that most references address computational models that are usually limited to an incompressible core, while ignoring all the localized effects involved as a result of the out of plane flexibility of the core. For all the static cases discussed geometrically linear analyses are considered, while for the dynamic cases nonlinear vibration analyses have been considered but still assuming an incompressible core and specific vibration modes.

In this paper, the principles of the HSAPT approach are used to determine the geometrically nonlinear response of a circular sandwich plate when subjected to a combination of mechanical and thermal loads, where the mechanical properties of the core material change with temperature. The computational model is based on the assumption of large displacements and moderate rotations with negligible shear deformations and linear constitutive relations for the face sheets. The core is modeled as a 3D small deformation linear elastic continuum with shear and vertical normal rigidities that are assumed to be of finite value, while the in-plane radial, circumferential and shear rigidities are neglected; see [Frostig et al. 1992] and the study in [Santiuste et al. 2011]. In addition, the loads are applied to the face sheets only, while the thermal loads is applied to all constituents. Finally, the face sheets and core are assumed to be fully bonded, and the face-core interfaces are able to transfer both shear and vertical normal stresses accordingly.

The mathematical formulation presents first the field and governing equations along with the appropriate boundary conditions and the closed-form solutions for the core displacement and stress fields of

a circular sandwich plate with a general construction layout. This is followed by the formulation for the special case of a radially symmetric sandwich plate. Finally, a numerical study of the response of circular sandwich plates subjected to axisymmetric combined mechanical and thermal loads is presented. This includes response curves within the sandwich plate and equilibrium curves of temperature versus selected structural variables/quantities.

2. Mathematical formulation

The field equations and the boundary conditions are derived following the steps of the HSAPT approach. They are derived using the variational principle of extremum of the total potential energy as follows:

$$\delta(U + V) = 0 \tag{1}$$

where U is in the internal potential strain energy, V is is the potential energy of the external loads, and δ is the variational operator.

The internal potential energy of the circular sandwich plate expressed in polar coordinates reads:

$$
\begin{aligned}
\delta U = \sum_{j=t,b} \Bigg(& \int_0^{2\pi} \int_{R_i}^{R_o} \int_{-\frac{1}{2}d_j}^{\frac{1}{2}d_j} \big(\sigma_{rrj}(r,\theta,z_j)\delta\epsilon_{rrj}(r,\theta,z_j) + \sigma_{\theta\theta j}(r,\theta,z_j)\delta\epsilon_{\theta\theta j}(r,\theta,z_j) \\
& \qquad\qquad + \tau_{r\theta j}(r,\theta,z_j)\delta\gamma_{r\theta j}(r,\theta,z_j)\big)r\, dz_j\, dr\, d\theta \Bigg) \\
+ & \int_0^{2\pi} \int_{R_i}^{R_o} \int_0^c \big(\tau_{rzc}(r,\theta,z_c)\delta\gamma_{rzc}(r,\theta,z_c) + \tau_{\theta zc}(r,\theta,z_c)\delta\gamma_{\theta zc}(r,\theta,z_c) \\
& \qquad\qquad + \sigma_{zzc}(r,\theta,z_c)\delta\epsilon_{zzc}(r,\theta,z_c)\big)r\, dz_c\, dr\, d\theta, \tag{2}
\end{aligned}
$$

where $\sigma_{rrj}(r,\theta,z_j)$ and $\sigma_{\theta\theta j}(r,\theta,z_j)$ $(j=t,b)$ are the normal stresses in the radial and circumferential directions of the upper and the lower face sheets, respectively; $\epsilon_{rrj}(r,z_j)$ and $\epsilon_{\theta\theta j}(r,\theta,z_j)$ $(j=t,b)$ are the normal strains in the radial and circumferential directions of the face sheets, respectively; $\tau_{jzc}(r,\theta,z_c)$, and $\gamma_{jzc}(r,\theta,z_c)$ $(j=r,\theta)$ are the vertical shear stresses and the shear angle on the radial and circumferential faces of the core, respectively; $\sigma_{zzc}(r,\theta,z_c)$, and $\epsilon_{zzc}(r,\theta,z_c)$ are the vertical normal stresses and strains in the core, respectively; $R_j (j=i,o)$ are the inner and outer radii of the plate; c is the height of the core; $z_k(k=t,b,c)$ are the vertical coordinates of the face sheets measured from their centroid planes, and of the core measured from upper the face-core interface, respectively; r is the radial coordinate measured from center of plate, and finally θ is the circumferential coordinate measured positive in the counterclockwise direction. For geometry, sign conventions, coordinates, deformations and internal resultants, see Figure 1.

The variation of the potential energy of the external loads reads:

$$
\begin{aligned}
\delta V = -\int_0^{2\pi} \Bigg(& \sum_{j=t,b} \Bigg(\int_{R_i}^{R_o} \big(n_{rr_j}(r,\theta)\delta u_{0j}(r,\theta) + n_{\theta\theta_j}(r,\theta)\delta v_{0j}(r.\theta) + q_j(r,\theta)\delta w_j(r,\theta)\big)r\, dr \Bigg) \\
& + \sum_{R_e=R_i}^{R_o} \big(N_{rre_j}(R_e,\theta)\delta u_{0j}(R_e,\theta) + N_{r\theta e_j}(R_e,\theta)\delta v_{0j}(R_i,\theta) + P_{e_j}(R_e,\theta)\delta w_j(R_e,\theta) \\
& \qquad + M_{rre_j}(R_e,\theta)\delta w_{j,r}(R_e,\theta) + M_{r\theta e_j}(R_e,\theta)\delta w_{j,\theta}(R_e,\theta)\big)R_e \Bigg) d\theta, \tag{3}
\end{aligned}
$$

where n_{kk_j} and q_j ($k = r, \theta$; $j = t, b$) are the external distributed loads in-plane and the vertical distributed load, respectively, at the upper and the lower face sheets; u_{0j}, v_{0j} and w_j ($j = t, b$) are the in-plane displacements in the radial and circumferential directions, and the vertical displacements, respectively of the upper and lower face sheets, respectively; $D_m f(r, \theta)$ ($m = r, \theta$) denotes a derivative of the function $f(r, \theta)$ with respect to the m-th variable or a derivative at a specified location; N_{ne_j}, P_{ne_j} and M_{ne_j} ($n = rr, r\theta$ and $j = t, b$) are the external concentrated loads in the radial and circumferential directions, in the vertical direction and the external bending moments in the radial and circumferential directions at the upper and lower face sheets. For sign conventions and definitions of loads see Figure 1.

The displacement distributions through the face sheet thicknesses there are assumed to follow the Euler–Bernoulli assumption of negligible through-thickness shear deformations and they read ($j = t, b$):

$$u_j(r, \theta, z_j) = u_{0j}(r, \theta) - z_j \frac{\partial}{\partial r} w_j(r, \theta),$$

$$v_j(r, \theta, z_j) = v_{0j}(r, \theta) - z_j \frac{\partial}{\partial \theta} w_j(r, \theta),$$
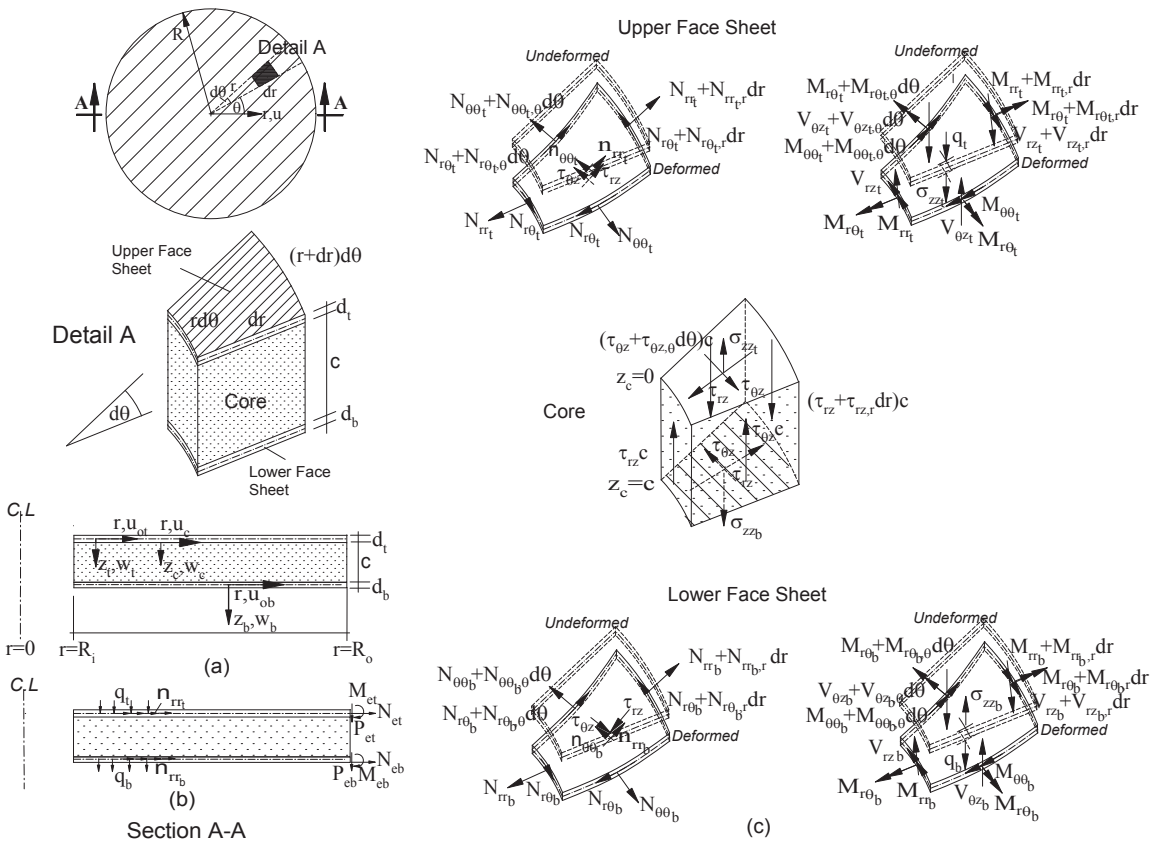
(4)

Figure 1. A typical circular sandwich plate: (a) plate layout, geometry and sign convention; (b) loads; (c) stress resultants in face sheets and core.

where u_{0j} and v_{0j} are the radial and circumferential displacements, respectively, of the mid-plane of the face sheets. Adopting the kinematic relations corresponding to moderately large deformations (von Kármán class of deformations), the radial and circumferential normal strains and the in-plane shear angle read ($j = t, b$):

$$\epsilon_{rrj}(r, \theta) = \epsilon_{rroj}(r, \theta) + z_j \chi_{rr_j}(r, \theta) - \alpha_j T_j(r, \theta, z_j),$$

$$\epsilon_{rroj}(r, \theta) = \frac{\partial}{\partial r} u_{0j}(r, \theta) + \frac{1}{2}\left(\frac{\partial}{\partial r} w_j(r, \theta)\right)^2,$$

$$\chi_{rj}(r, \theta) = -\frac{\partial^2}{\partial r^2} w_j(r, \theta),$$

$$\epsilon_{\theta\theta j}(r, \theta) = \epsilon_{\theta\theta oj}(r, \theta) + z_j \chi_{\theta\theta_j}(r, \theta) - \alpha_j T_j(r, \theta, z_j),$$

$$\epsilon_{\theta\theta oj}(r, \theta) = \frac{1}{r} u_{0j}(r, \theta) + \frac{1}{r}\frac{\partial}{\partial\theta} v_{0j}(r, \theta) + \frac{1}{2r^2}\left(\frac{\partial}{\partial\theta} w_j(r, \theta)\right)^2, \qquad (5)$$

$$\chi_{\theta\theta_j}(r, \theta) = -\frac{1}{r}\frac{\partial}{\partial r} w_j(r, \theta) - \frac{1}{r^2}\frac{\partial^2}{\partial\theta^2} w_j(r, \theta),$$

$$\gamma_{r\theta_j}(r, \theta) = \gamma_{r\theta oj}(r, \theta) + z_j \chi_{r\theta_j}(r, \theta),$$

$$\gamma_{r\theta oj}(r, \theta) = \frac{1}{r}\frac{\partial}{\partial\theta} u_{0j}(r, \theta) - \frac{1}{r} v_{0j}(r, \theta) + \frac{\partial}{\partial r} v_{0j}(r, \theta) + \frac{1}{r}\frac{\partial}{\partial r} w_j(r, \theta)\frac{\partial}{\partial\theta} w_j(r, \theta),$$

$$\chi_{r\theta_j}(r, \theta) = -\frac{2}{r}\frac{\partial^2}{\partial\theta\,\partial r} w_j(r, \theta) + \frac{2}{r^2}\frac{\partial}{\partial\theta} w_j(r, \theta),$$

where ϵ_{kko_j} ($k = r, \theta$) denotes the mid-plane strains in the radial and circumferential directions, $\gamma_{r\theta o_j}$ ($j = t, b$) the in-plane shear angles of the top and bottom face sheets, χ_{kl_j} ($k, l = r, \theta$) the radial, circumferential and twist curvatures, the temperature distribution through the depth of the (top or bottom) face sheet reads,

$$T_j(r, \theta, z_j) = \frac{1}{2}\big(T_{jb}(r, \theta) + T_{jt}(r, \theta)\big) + \frac{z_j}{h}\big(T_{jb}(r, \theta) - T_{jt}(r, \theta)\big) \quad (j = t, b), \qquad (6)$$

and α_j ($j = t, b$) the coefficient of thermal expansion of the face sheet.

The kinematic relations of the core material are derived assuming small displacements and rotations, and they read

$$\gamma_{rzc}(r, \theta, z_c) = \frac{\partial}{\partial z_c} u_c(r, \theta, z_c) + \frac{\partial}{\partial r} w_c(r, \theta, z_c),$$

$$\gamma_{\theta zc}(r, \theta, z_c) = \frac{\partial}{\partial z_c} v_c(r, \theta, z_c) + \frac{\partial}{\partial\theta} w_c(r, \theta, z_c), \qquad (7)$$

$$\epsilon_{zzc}(r, \theta, z_c) = \frac{\partial}{\partial z_c} w_c(r, \theta, z_c) - \alpha_c T(r, \theta, z_c),$$

where $u_c(r, \theta, z_c)$, $v_c(r, \theta, z_c)$ and $w_c(r, \theta, z_c)$ are the radial, circumferential and vertical core displacements, respectively.

The compatibility conditions corresponding to perfect bonding between the face sheets and the core require that the following conditions are fulfilled:

$$u_c(r, \theta, z_{cj}) = u_{0j}(r, \theta) + \tfrac{1}{2}(-1)^k d_j \frac{\partial}{\partial r} w_j(r, \theta),$$

$$v_c(r, \theta, z_{cj}) = v_{0j}(r, \theta) + \tfrac{1}{2}(-1)^k d_j \frac{\partial}{\partial \theta} w_j(r, \theta), \qquad (8)$$

$$w_c(r, \theta, z_{cj}) = w_j(r, \theta),$$

where $k = 1$ when $j = t$, $k = 0$ when $j = b$, and z_{cj} $(j = t, b)$ are the vertical coordinates at the upper and the lower face-core interfaces, respectively; thus $z_{ct} = 0$ and $z_{cb} = c$. See Figure 1 for coordinate definitions for the core.

The field equations and the boundary conditions are derived using the variational principle (1), the variational energies (2) and (3), the kinematic relations (5)–(7) of the face sheets and the core, the compatibility requirements (8), and the stress resultants (see Figure 1).

Hence, after integration by parts and some algebraic manipulations, the field equations for the face sheets $(j = t, b)$ read:

$$-\frac{\partial}{\partial \theta} N_{r\theta_j}(r, \theta) + N_{\theta\theta_j}(r, \theta) - N_{rr_j}(r, \theta) - r\frac{\partial}{\partial r} N_{rr_j}(r, \theta) - rn_{rr_j}(r, \theta) + (-1)^k r\tau_{rz_j}(r, \theta) = 0,$$

$$-2N_{r\theta_j}(r, \theta) - \frac{\partial}{\partial \theta} N_{\theta\theta_j}(r, \theta) - rn_{\theta\theta_j}(r, \theta) - r\frac{\partial}{\partial r} N_{r\theta_j}(r, \theta) + (-1)^k r\tau_{\theta z_j}(r, \theta) = 0,$$

$$r\frac{\partial}{\partial \theta} m_{\theta\theta_j}(r, \theta) + \frac{\partial}{\partial r} M_{\theta\theta_j}(r, \theta) - \frac{2}{r}\frac{\partial}{\partial \theta} M_{r\theta_j}(r, \theta) - \frac{d_j}{2}\left(r\frac{\partial}{\partial \theta}\tau_{\theta zc_j}(r, \theta) + r\frac{\partial}{\partial r}\tau_{rzc_j}(r, \theta) + \tau_{rzc_j}(r, \theta)\right)$$

$$+ \left((-1)^{k-1} r\tau_{rzc_j}(r, \theta) + rn_{rr_j}(r, \theta) - N_{\theta\theta_j}(r, \theta)\right)\frac{\partial}{\partial r} w_j(r, \theta)$$

$$+ \left((-1)^{k-1}\tau_{\theta zc_j}(r, \theta) + n_{\theta\theta_j}(r, \theta) + \frac{2}{r}N_{r\theta_j}(r, \theta)\right)\frac{\partial}{\partial \theta} w_j(r, \theta)$$

$$- 2N_{r\theta_j}(r, \theta)\frac{\partial^2}{\partial \theta \partial r} w_j(r, \theta) - rq_j(r, \theta) + (-1)^k r\sigma_{zzj}(r, \theta) - \frac{1}{r}\frac{\partial^2}{\partial \theta^2} M_{\theta\theta_j}(r, \theta) - r\frac{\partial^2}{\partial r^2} M_{rr_j}(r, \theta)$$

$$- rN_{rr_j}(r, \theta)\frac{\partial^2}{\partial r^2} w_j(r, \theta) - \frac{1}{r}N_{\theta\theta_j}(r, \theta)\frac{\partial^2}{\partial \theta^2} w_j(r, \theta) - 2\frac{\partial^2}{\partial \theta \partial r} M_{r\theta_j}(r, \theta) - 2\frac{\partial}{\partial r} M_{rr_j}(r, \theta) = 0, \quad (9)$$

where $k = 1, 2$ indicate the upper and the lower face-core interfaces, respectively; N_{rr_j}, $N_{\theta\theta_j}$ and $N_{r\theta_j}$ $(j = t, b)$ are respectively the in-plane stress resultants in the radial and circumferential directions and the in-plane shear stress resultants of the face sheets; M_{rr_j}, $M_{\theta\theta_j}$ and $M_{r\theta_j}$ $(j = t, b)$ are the bending moment resultants in the radial and circumferential directions and the torsion moment resultants of the face sheets; τ_{rzc_j} and $\tau_{\theta zc_j}$ $(j = t, b)$ are the radial and circumferential core shear stresses at the upper and the interfaces of the core, respectively, and σ_{zzcj} are the vertical normal stresses at the upper and the lower face core interfaces, respectively. It should be noticed that the core shear stresses in the circumferential direction are null when no in-plane distributed loads are applied; see second equation in (9).

The field equations for the core read:

$$\frac{\partial}{\partial z_c}\tau_{rzc}(r,\theta,z_c)=0, \qquad \frac{\partial}{\partial z_c}\tau_{\theta zc}(r,\theta,z_c)=0,$$

$$r\frac{\partial}{\partial z_c}\sigma_{zzc}(r,\theta,z_c)+r\frac{\partial}{\partial r}\tau_{rzc}(r,\theta,z_c)+\tau_{rzc}(r,\theta,z_c)-r\frac{\partial}{\partial\theta}\tau_{\theta zc}(r,\theta,z_c)=0. \tag{10}$$

It should be noticed that due to the geometrical nonlinearities of the face sheets, the equilibrium conditions on each differential segment of the face sheets and the core, which equal to the field equations, should be conducted on the deformed shape of the face sheets, and the undeformed shape of the core; see Figure 1.

The boundary conditions at the inner and outer edges of the face sheets and the core (i.e., at $r=R_i$ and R_o) of the circular sandwich plate are given below.

The boundary conditions for the face sheets ($j=t,b$) read:

$$\lambda N_{rr_j}(R_k,\theta)-N_{re_j}(R_k,\theta)=0 \qquad \text{or} \qquad u_{0j}(R_k,\theta)-u_{0e_j}(R_k,\theta)=0,$$

$$\lambda N_{r\theta_j}(R_e,\theta)-N_{r\theta e_j}(R_e,\theta)=0 \qquad \text{or} \qquad v_{0j}(R_k,\theta)-v_{0e_j}(R_k,\theta)=0,$$

$$-M_{re_j}(R_k,\theta)-\lambda M_{rr_j}(R_k,\theta)=0 \qquad \text{or} \qquad Dw_j(R_k,\theta)-Dw_{ej}(R_k,\theta)=0,$$

$$\lambda\big(R_e N_{rr_j}(R_e,\theta)D_r w_j(R_e,\theta)+D_r M_{rr_j}(R_e,\theta)R_e$$
$$+\tfrac{1}{2}d_j\tau_r(R_e,\theta)R_e+N_{r\theta_j}(R_e,\theta)D_\theta(w_j)(R_e,\theta)$$
$$+2D_\theta(M_{r\theta_j})(R_e,\theta)-M_{\theta\theta_j}(R_e,\theta)+M_{rr_j}(R_e,\theta)\big)$$
$$+D_\theta(M_{r\theta e_j})(R_e,\theta)R_e-P_{e_j}(R_e,\theta)R_e=0 \qquad \text{or} \qquad w_j(R_k,\theta)-w_{e_j}(R_k,\theta)=0, \tag{11}$$

where $\lambda=1$ when $r=R_o$ and $\lambda=-1$ when $r=R_i$; $k=o$ or i; u_{0e_j}, v_{0e_j}, Dw_{e_j} and w_{e_j} ($j=t,b$) are the prescribed radial, circumferential, radial rotations and vertical displacements at the edges of the upper and the lower face sheet, respectively; N_{re_j}, $N_{r\theta e_j}$ ($j=t,b$)are the external imposed radial and circumferential loads (stress resultants); M_{re_j} and $M_{r\theta e_j}$ ($j=t,b$) are the bending and twist moment resultants in the radial and circumferential directions, respectively, imposed at the edges of the face sheets; and

$$D_k(f)(R_l,\theta)=\frac{\partial}{\partial k}f(r,\theta)|_{r=R_l} \quad (k=r,\theta; \; l=i,o)$$

is the derivative of the function f at the edge of the panel.

The boundary conditions for the core read:

$$\tau_{rzc}(R_k,\theta)=0 \quad \text{or} \quad w_c(R_k,\theta,z_c)-w_{ec}(R_k,\theta,z_c)=0, \tag{12}$$

where $w_{ec}(R_k,\theta,z_c)$ are the prescribed vertical core displacements at the edge of the sandwich plate with a specified distribution through the depth of the core.

In order to express the governing equations in explicit form, the core stress and displacement fields must be defined first. This will be derived next for a core with uniform mechanical properties that are temperature-independent (TI).

3. Core fields — uniform mechanical properties (TI)

The explicit formulation of the isotropic core stress and displacement fields is achieved by using the kinematic relations (7), the compatibility conditions (8) and the constitutive relations

$$\epsilon_{zzc}(r, \theta, z_c) = \frac{\sigma_{zzc}(r, \theta, z_c)}{E_{zc}} + \alpha_c T_c(r, \theta, z_c),$$

$$\gamma_{rzc}(r, \theta, z_c) = \frac{\tau_{rzc}(r, \theta)}{G_{rzc}}, \quad \gamma_{\theta zc}(r, \theta, z_c) = \frac{\tau_{\theta zc}(r, \theta)}{G_{\theta zc}}, \tag{13}$$

where E_{zc}, G_{rzc} and $G_{\theta zc}$ are the vertical modulus of elasticity and the shear moduli of the core in the radial and circumferential directions, respectively; and $T_c(r, \theta, z_c)$ is the temperature field within the core imposed throughout the sandwich plate.

The stress field within the core is derived through the solution of the field equations (10) of the core. Hence they read:

$$\tau_{rzc}(r, \theta, z_c) = \tau_r(r, \theta), \qquad \tau_{\theta zc}(r, \theta, z_c) = \tau_\theta(r, \theta),$$

$$\sigma_{zzc}(r, \theta, z_c) = -z_c \frac{\partial}{\partial r} \tau_r(r, \theta) - z_c \frac{1}{r} \tau_r(r, \theta) - z_c \frac{\partial}{\partial \theta} \tau_\theta(r, \theta) + C_{w1}(r, \theta), \tag{14}$$

where $C_{w1}(r, \theta)$ is a coefficient of integration to be determined through the compatibility conditions at the face-core interfaces; see third equation in (8).

The displacements fields of the core in the radial and circumferential directions are determined through the constitutive relations (13), and by enforcing four compatibility conditions (8); in the radial and circumferential directions at the upper face-core interface, respectively, and in the vertical direction at the upper and the lower interfaces, respectively. The temperature field is assumed to be radially symmetric for simplicity and linear through the depth of the core.

After some algebraic manipulations the explicit description of the radial stress and displacements fields in the core read:

$$\sigma_{zzc}(r, \theta) = -\tfrac{1}{2} E_{zc} \big(T_{cb}(r) + T_{ct}(r) \big) \alpha_c + \frac{1}{c} E_{zc} \big(w_b(r, \theta) - w_t(r, \theta) \big)$$
$$+ \tfrac{1}{2}(-2z_{cj} + c) \Big(\frac{\partial}{\partial r} \tau_r(r, \theta) + \frac{\partial}{\partial \theta} \tau_\theta(r, \theta) + \frac{1}{r} \tau_r(r, \theta) \Big),$$

$$w_c(r, \theta, z_c) = -\frac{z_c}{2c}(-z_c + c) \big(T_{cb}(r) - T_{ct}(r) \big) \alpha_c + \frac{z_c}{c} w_b(r, \theta) + \Big(1 - \frac{z_c}{c} \Big) w_t(r, \theta)$$
$$+ \frac{1}{2E_{zc}} z_c(-z_c + c) \Big(\frac{\partial}{\partial r} \tau_r(r, \theta) + \frac{\partial}{\partial \theta} \tau_\theta(r, \theta) + \frac{1}{r} \tau_r(r, \theta) \Big),$$

$$u_c(r, \theta, z_c) = -\frac{z_c^2(3c - 2z_c)}{12c} \frac{d}{dr} \big(T_{ct}(r) - T_{cb}(r) \big) \alpha_c - \frac{z_c^2}{2c} \frac{\partial}{\partial r} w_b(r, \theta) + \Big(\frac{z_c^2}{2c} - z_c - \frac{d_t}{2} \Big) \frac{\partial}{\partial r} w_t(r, \theta)$$
$$- \frac{z_c^2(3c - 2z_c)}{12E_{zc}r^2} \Big(r^2 \frac{\partial^2}{\partial r^2} \tau_r(r, \theta) + r^2 \frac{\partial^2}{\partial \theta \partial r} \tau_\theta(r, \theta) + r \frac{\partial}{\partial r} \tau_r(r, \theta) - \tau_r(r, \theta) \Big) + \frac{z_c}{G_{rzc}} \tau_r(r, \theta) + u_{0t}(r, \theta),$$

$$v_c(r, \theta, z_c) = -\frac{z_c^2}{2c} \frac{\partial}{\partial \theta} w_b(r, \theta) + \Big(\frac{z_c^2}{2c} - z_c - \frac{d_t}{2} \Big) \frac{\partial}{\partial \theta} w_t(r, \theta)$$
$$- \frac{z_c^2(3c - 2z_c)}{12E_{zc}r} \Big(r \frac{\partial^2}{\partial \theta^2} \tau_\theta(r, \theta) + \frac{\partial}{\partial \theta} \tau_r(r, \theta) + r \frac{\partial^2}{\partial \theta \partial r} \tau_r(r, \theta) \Big) + \frac{z_c}{G_{\theta zc}} \tau_\theta(r, \theta) + v_{0t}(r, \theta), \tag{15}$$

Notice that the distribution, through the depth of the core, of the vertical normal stresses is linear, that of the vertical displacement is quadratic and those of the radial and circumferential displacements are cubic. In addition, the circumferential displacements are shown to be independent of the temperature due to the assumption of a radially symmetric thermal field.

4. Nonlinear governing equations

The governing equations are derived assuming that the face sheets are linear elastic and isotropic, and that the core is linear, elastic and orthotropic. Hence, the nonlinear stress resultant-displacement relations for the face sheets ($j = t, b$) can be expressed in the form:

$$N_{rr_j}(r, \theta) = \mathbb{A}_j \left(\frac{\partial}{\partial r} u_{0j}(r, \theta) + \frac{1}{2} \left(\frac{\partial}{\partial r} w_j(r, \theta) \right)^2 - \frac{1}{2} \alpha_j (1 + \mu_j) \left(T_{jt}(r) + T_{jb}(r) \right) \right.$$
$$\left. + \mu_j \left(\frac{1}{r} u_{0j}(r, \theta) + \frac{1}{r} \frac{\partial}{\partial \theta} v_{0j}(r, \theta) + \frac{1}{2r^2} \left(\frac{\partial}{\partial \theta} w_j(r, \theta) \right)^2 \right) \right),$$

$$N_{\theta\theta_j}(r, \theta) = \mathbb{A}_j \left(\frac{1}{r} u_{0j}(r, \theta) + \frac{1}{r} \frac{\partial}{\partial \theta} v_{0j}(r, \theta) + \frac{1}{2r^2} \left(\frac{\partial}{\partial \theta} w_j(r, \theta) \right)^2 \right.$$
$$\left. - \frac{1}{2} \alpha_j (1 + \mu_j) \left(T_{jt}(r) + T_{jb}(r) \right) + \mu_j \left(\frac{\partial}{\partial r} u_{0j}(r, \theta) + \frac{1}{2} \left(\frac{\partial}{\partial r} w_j(r, \theta) \right)^2 \right) \right),$$

$$N_{r\theta_j}(r, \theta) = \frac{1}{2} \mathbb{A}_j (1 - \mu_j) \left(\frac{1}{r} \frac{\partial}{\partial \theta} u_{0j}(r, \theta) - \frac{1}{r} v_{0j}(r, \theta) + \frac{\partial}{\partial r} v_{0j}(r, \theta) + \frac{1}{r} \frac{\partial}{\partial r} w_j(r, \theta) \frac{\partial}{\partial \theta} w_j(r, \theta) \right),$$

$$M_{rr_j}(r, \theta) = \mathbb{D}_j \left(-\frac{\partial^2}{\partial r^2} w_j(r, \theta) - \frac{\alpha_j}{d_j} \left(T_{jt}(r) - T_{jb}(r) \right) (1 + \mu_j) - \frac{\mu_j}{r} \frac{\partial}{\partial r} w_j(r, \theta) - \frac{\mu_j}{r^2} \frac{\partial^2}{\partial \theta^2} w_j(r, \theta) \right),$$

$$M_{\theta\theta_j}(r, \theta) = \mathbb{D}_j \left(-\frac{1}{r} \frac{\partial}{\partial r} w_j(r, \theta) - \frac{1}{r^2} \frac{\partial^2}{\partial \theta^2} w_j(r, \theta) - \frac{\alpha_j}{d_j} \left(T_{jt}(r) - T_{jb}(r) \right) (1 + \mu_j) - \mu_j \frac{\partial^2}{\partial r^2} w_j(r, \theta) \right),$$

$$M_{r\theta_j}(r, \theta) = \mathbb{D}_j (1 - \mu_j) \left(-\frac{2}{r} \left(\frac{\partial^2}{\partial \theta \partial r} w_j(r, \theta) \right) + \frac{2}{r^2} \left(\frac{\partial}{\partial \theta} w_j(r, \theta) \right) \right). \tag{16}$$

Here μ_j ($j = t, b$) is the Poisson's ratio for the face sheets and $\mathbb{A}_j$, $\mathbb{D}_j$ ($j = t, b$) are the in-plane and flexural rigidities, respectively, which are given by

$$\mathbb{A}_j = \frac{E_j d_j}{1 - \mu_j^2},$$

$$\mathbb{D}_j = \frac{E_j d_j^3}{12(1 - \mu_j^2)}.$$

The governing equations are derived through substitution of the stress resultant-displacements relations (16) of the face sheets into the field equations (9), and the compatibility conditions — given in the first and second equations in (8) — between the core and the lower face sheet in the radial and circumferential directions, which combined with the core displacement field (15) yield two compatibility equations.

Hence, the governing equations for the face sheets after some algebraic manipulations read ($j = t, b$):

$$\mathbb{A}_j \Bigg(\frac{1}{2} r(1+\mu_j)\alpha_j \frac{d}{dr}\big(T_{jt}(r) + T_{jb}(r)\big)$$

$$+ \frac{1}{2}(\mu_j - 1)\bigg(\Big(\frac{\partial}{\partial r} w_j(r,\theta)\Big)^2 + \frac{1}{r}\frac{\partial^2}{\partial \theta^2} u_{0j}(r,\theta) + \frac{1}{r}\frac{\partial^2}{\partial \theta^2} w_j(r,\theta) \frac{\partial}{\partial r} w_j(r,\theta) \bigg)$$

$$- \frac{1}{2}(1+\mu_j)\bigg(-\frac{1}{r^2}\Big(\frac{\partial}{\partial \theta} w_j(r,\theta)\Big)^2 + \frac{\partial^2}{\partial \theta \, \partial r} v_{0j}(r,\theta) + \frac{1}{r}\frac{\partial^2}{\partial \theta \, \partial r} w_j(r,\theta) \frac{\partial}{\partial \theta} w_j(r,\theta) \bigg)$$

$$- r\frac{\partial^2}{\partial r^2} u_{0j}(r,\theta) - r\frac{\partial}{\partial r} w_j(r,\theta) \frac{\partial^2}{\partial r^2} w_j(r,\theta) - \frac{1}{2r}(-3+\mu_j)\frac{\partial}{\partial \theta} v_{0j}(r,\theta) + \frac{1}{r}u_{0j}(r,\theta) - \frac{\partial}{\partial r} u_{0j}(r,\theta) \bigg)$$

$$+ (-1)^k r\tau_r(r,\theta) - rn_{rr_j}(r,\theta) = 0,$$

$$\mathbb{A}_j \Bigg(-\frac{1}{2}(1+\mu_j)\bigg(\frac{\partial^2}{\partial \theta \, \partial r} u_{0j}(r,\theta) + \frac{\partial^2}{\partial \theta \, \partial r} w_j(r,\theta) \frac{\partial}{\partial r} w_j(r,\theta) \bigg)$$

$$+ \frac{1}{2}(\mu_j - 1)\bigg(\frac{\partial}{\partial \theta} w_j(r,\theta)\Big(\frac{\partial^2}{\partial r^2} w_j(r,\theta) + \frac{1}{r}\frac{\partial}{\partial r} w_j(r,\theta)\Big) + r\frac{\partial^2}{\partial r^2} v_{0j}(r,\theta) - \frac{1}{r^2}v_{0j}(r,\theta) + \frac{1}{r}\frac{\partial}{\partial r} v_{0j}(r,\theta) \bigg)$$

$$- \frac{1}{r}\frac{\partial^2}{\partial \theta^2} v_{0j}(r,\theta) - \frac{1}{r^2}\frac{\partial}{\partial \theta} w_j(r,\theta) \frac{\partial^2}{\partial \theta^2} w_j(r,\theta) + \frac{1}{2r}(-3+\mu_j)\frac{\partial}{\partial \theta} u_{0j}(r,\theta) \Bigg) + (-1)^k r\tau_\theta(r,\theta) - rn_{\theta\theta_j}(r,\theta) = 0,$$

$$-\frac{\alpha_j}{d_j}\mathbb{D}_j(\mu_j + 1)\bigg(r\frac{d^2}{dr^2}\big(T_{jb}(r) - T_{jt}(r)\big) + \frac{d}{dr}\big(T_{jb}(r) - T_{jb}(r)\big) \bigg) + \mathbb{D}_j r\frac{\partial^4}{\partial r^4} w_j(r,\theta) + \frac{\mathbb{D}_j}{r^3}\frac{\partial^4}{\partial \theta^4} w_j(r,\theta) + 2\mathbb{D}_j \frac{\partial^3}{\partial r^3} w_j(r,\theta)$$

$$+ \big(n_{\theta\theta_j}(r,\theta) + \tau_t(r,\theta)\big)\frac{\partial}{\partial \theta} w_j(r,\theta) + (-1)^k r\sigma_{zzj}(r,\theta) - rq_j(r,\theta) + r\frac{\partial}{\partial \theta} m_{\theta\theta_j}(r,\theta) + r\frac{\partial}{\partial r} m_{rr_j}(r,\theta)$$

$$+ \frac{1}{2r^3}\bigg(\Big(-2r\Big(\mu_j r\frac{\partial}{\partial r} u_{0j}(r,\theta) + \frac{\partial}{\partial \theta} v_{0j}(r,\theta) + u_{0j}(r,\theta)\Big) + r^2 \alpha_j(\mu_j + 1)\big(T_{jt}(r) + T_{jb}(r)\big)\Big)\mathbb{A}_j - 4\mathbb{D}_j(\mu_j - 3) \bigg)\frac{\partial^2}{\partial \theta^2} w_j(r,\theta)$$

$$- \frac{1}{2}\mathbb{A}_j\bigg(r\Big(\frac{\partial}{\partial r} w_j(r,\theta)\Big)^2 \frac{\partial^2}{\partial r^2} w_j(r,\theta) + \frac{1}{r^3}\Big(\frac{\partial}{\partial \theta} w_j(r,\theta)\Big)^2 \frac{\partial^2}{\partial \theta^2} w_j(r,\theta) \bigg)$$

$$- \frac{1}{2}\mathbb{A}_j \mu_j\bigg(\Big(\frac{\partial}{\partial r} w_j(r,\theta)\Big)^3 + \frac{1}{r}\Big(\frac{\partial}{\partial r} w_j(r,\theta)\Big)^2 \frac{\partial^2}{\partial \theta^2} w_j(r,\theta) + \frac{1}{r}\Big(\frac{\partial}{\partial \theta} w_j(r,\theta)\Big)^2 \frac{\partial^2}{\partial r^2} w_j(r,\theta) \bigg)$$

$$+ \bigg(\mathbb{A}_j\Big(\frac{\mu_j+1}{2}\big(T_{jt}(r) + T_{jb}(r)\big)\alpha_j - \frac{2\mu_j - 1}{2r^2}\Big(\frac{\partial}{\partial \theta} w_j(r,\theta)\Big)^2 - \frac{1}{r}\frac{\partial}{\partial \theta} v_{0j}(r,\theta) $$

$$- \frac{1}{r}u_{0j}(r,\theta) + \frac{\mu_j - 1}{r}\frac{\partial^2}{\partial \theta \, \partial r} w_j(r,\theta) \frac{\partial}{\partial \theta} w_j(r,\theta) - \mu_j \frac{\partial}{\partial r} u_{0j}(r,\theta) \Big) + r\tau_r(r,\theta) + rn_{rr_j}(r,\theta) + \frac{\mathbb{D}_j}{r^2} \bigg)\frac{\partial}{\partial r} w_j(r,\theta)$$

$$+ \frac{1}{r^2}\bigg(\mathbb{A}_j(\mu_j - 1)\Big(r\frac{\partial}{\partial r} v_{0j}(r,\theta) - v_{0j}(r,\theta) + \frac{\partial}{\partial \theta} u_{0j}(r,\theta)\Big)\Big(r\frac{\partial^2}{\partial \theta \, \partial r} w_j(r,\theta) - \frac{\partial}{\partial \theta} w_j(r,\theta)\Big) \bigg)$$

$$+ \frac{2}{r^2}\mathbb{D}_j(\mu_j - 2)\bigg(\frac{\partial^3}{\partial \theta^2 \partial r} w_j(r,\theta) - r\frac{\partial^4}{\partial \theta^2 \partial r^2} w_j(r,\theta) \bigg)$$

$$- \bigg(\mathbb{A}_j\Big(r\frac{\partial}{\partial r} u_{0j}(r,\theta) + \mu_j \frac{\partial}{\partial \theta} v_{0j}(r,\theta) + \mu_j u_{0j}(r,\theta) - \frac{\mu_j + 1}{2} r\alpha_j\big(T_{jt}(r) + T_{jb}(r)\big) \Big) + \frac{\mathbb{D}_j}{r} \bigg)\frac{\partial^2}{\partial r^2} w_j(r,\theta)$$

$$+ m_{rr_j}(r,\theta) - \frac{1}{2}d_j\Big(\tau_r(r,\theta) + r\frac{\partial}{\partial r}\tau_r(r,\theta) + r\frac{\partial}{\partial \theta}\tau_\theta(r,\theta) \Big) = 0. \quad (17)$$

The two corresponding resulting compatibility equations read:

$$-\frac{1}{12}c^2\frac{d}{dr}\big(T_{ct}(r)-T_{cb}(r)\big)\alpha_c-\frac{1}{2}(c+d_b)\frac{\partial}{\partial r}w_b(r,\theta)-\frac{1}{2}(c+d_t)\frac{\partial}{\partial r}w_t(r,\theta)+u_{0t}(r,\theta)-u_{0b}(r,\theta)$$

$$+\left(\frac{c}{G_{rzc}}+\frac{1}{12}\frac{c^3}{E_{zc}r^2}\right)\tau_r(r,\theta)-\frac{c^3}{12E_{zc}}\left(\frac{1}{r}\frac{\partial}{\partial r}\tau_r(r,\theta)+\frac{\partial^2}{\partial r^2}\tau_r(r,\theta)+\frac{\partial^2}{\partial\theta\,\partial r}\tau_\theta(r,\theta)\right)=0,$$

$$-\frac{1}{2}(c+d_b)\frac{\partial}{\partial\theta}w_b(r,\theta)-\frac{1}{2}(c+d_t)\frac{\partial}{\partial\theta}w_t(r,\theta)+\frac{\tau_\theta(r,\theta)c}{G_{\theta zc}}+v_{0t}(r,\theta)-v_{0b}(r,\theta)$$

$$-\frac{c^3}{12E_{zc}}\left(\frac{1}{r}\frac{\partial}{\partial\theta}\tau_r(r,\theta)+\frac{\partial^2}{\partial\theta^2}\tau_t(r,\theta)+\frac{\partial^2}{\partial\theta\,\partial r}\tau_r(r,\theta)\right)=0, \quad (18)$$

where $k=1,2$ correspond to the upper and the lower face-core interfaces, respectively.

The unknowns in the set of the governing equations (or the fundamental variables of the problem) consist of the in-plane radial and circumferential displacements (u_{0j} and v_{0j}) and the vertical displacement (w_j) of the two face sheets ($j=t,b$), and the two core shear stresses in the radial and circumferential directions (τ_r, τ_θ), respectively. Thus the order of the set of partial differential equations (PDEs) includes two for the in-plane displacements of each face sheets and shear stresses in the core, and four for the vertical displacements of each face sheet. Hence, the total order of the complete set of PDEs is 18, which corresponds exactly to the number of boundary conditions to be imposed at the edges of sandwich plate including both the face sheets and the core; see Equations (11) for the face sheets and Equations (12) for the core.

The general solution to the set of nonlinear PDEs and the corresponding boundary conditions may be reduced to a set of nonlinear ordinary differential equations (ODEs) through the use of methods such as Kantorovich, Galerkin or similar approaches with the aid of periodic functions in the circumferential direction; see for example [Rabinovitch and Frostig 2002a]. In order to understand the effects of the main parameters on the nonlinear thermomechanical response including degradation of the mechanical core properties with increasing temperature, the special case of a radially symmetric (or axisymmetric) circular sandwich plate is studied next.

5. Radially symmetric sandwich plates — nonlinear governing equations

The case of radially symmetric sandwich plates requires that the mechanical properties of all constituents are dependent on the radial coordinate only, that the loads (mechanical and thermal) scheme is radially symmetric, and that the imposed boundary conditions do not depend on the circumferential coordinate. Accordingly, all the dependent variables of the problem must be functions of the radial coordinate only. For completeness, the field equations, constitutive relations and the explicit description of the governing equations for the case of radially symmetric panel is presented in the following.

The field equations for the face sheets ($j=t,b$) are:

$$-rn_{rr_j}(r)-r\frac{d}{dr}N_{rr_j}(r)+(-1)^k r\tau_{rzc_j}(r)+N_{\theta\theta_j}(r)-N_{rr_j}(r)=0, \qquad (-1)^k\tau_{\theta zc_j}(r)-n_{\theta\theta_j}(r)=0,$$

$$\left((-1)^{k-1}r\frac{d}{dr}w_j(r)-\frac{d_j}{2}\right)\tau_{rzc_j}(r)-\frac{d_j}{2}r\frac{d}{dr}\tau_{rzc_j}(r)+\big(rn_{rr_j}(r)-N_{\theta\theta_j}(r)\big)\frac{d}{dr}w_j(r)+\frac{d}{dr}M_{\theta\theta_j}(r)$$

$$+(-1)^k r\sigma_{zzcj}(r)-rN_{rr_j}(r)\frac{d^2}{dr^2}w_j(r)-rq_j(r)-2\frac{d}{dr}M_{rr_j}(r)-r\frac{d^2}{dr^2}M_{rr_j}(r)=0, \quad (19)$$

where $k = 1, 2$ for the upper and the lower face-core interfaces respectively. Please notice that if no radial in-plane external loads is imposed, then the circumferential shear stresses within the core are zero. Hence the number of equations reduces to two for each face sheet.

The number of boundary conditions at the inner and outer plate radii, R_i, and R_o, changes to three for each face sheet as follows ($j = t, b$):

$$\lambda N_{rr_j}(R_k) - N_{re_j}(R_k) = 0 \quad \text{or} \quad u_{0j}(R_k) - u_{0ej}(R_k) = 0$$

$$\lambda M_{rr_j}(R_k) + M_{re_j}(R_k) = 0 \quad \text{or} \quad Dw_j(R_k) - Dw_{ej}(R_k) = 0$$

$$\lambda \Big(R_j N_{rr_j}(R_k) D(w_j)(R_k) - R_k m_{rr_j}(R_k)$$
$$+ R_j DM_{rr_j}(R_k) + \tfrac{1}{2} d_j R_j \tau_{rzc_j}(R_k)$$
$$+ M_{rr_j}(R_k) - M_{\theta\theta_j}(R_k) \Big) - R_j P_{e_j}(R_k) = 0 \quad \text{or} \quad w_j(R_k) - w_{e_j}(R_k) = 0 \quad (20)$$

where $\lambda = 1$ for $r = R_o$ and $\lambda = -1$ for $r = R_i$; $k = o$ or i. Notice that due to the radially symmetric constraints there are no boundary conditions imposed with respect to loads and displacements in the circumferential direction.

The stress resultant-displacement relations read:

$$N_{rr_j}(r) = \mathbb{A}_j \Big(-\frac{1}{2}(1 + \mu_j)\big(T_{jt}(r) + T_{jb}(r)\big)\alpha_j + \frac{d}{dr}u_{0j}(r) + \frac{1}{2}\Big(\frac{d}{dr}w_j(r)\Big)^2 + \frac{1}{r}\mu_j u_{0j}(r)j \Big),$$

$$M_{rr_j}(r) = \mathbb{D}_j \Big(-\frac{1}{d_j}(1 + \mu_j)\big(T_{jt}(r) - T_{jb}(r)\big)\alpha_j + \frac{d^2}{dr^2}w_j(r) + \frac{1}{r}\mu_j \frac{d}{dr}w_j(r) \Big),$$

$$N_{\theta\theta_j}(r) = \mathbb{A}_j \Big(\frac{1}{2}\alpha_j(\mu_j^2 - 1)\big(T_{jt}(r) + T_{jb}(r)\big) + \frac{1}{r}(1 - \mu_j^2)u_{0j}(r) \Big) + \mu_j N_{rr_j}(r),$$

$$M_{\theta\theta_j}(r) = \mathbb{D}_j \Big(\frac{\alpha_j}{d_j}\big(T_{jt}(r) - T_{jb}(r)\big)(\mu_j^2 - 1) + \frac{1}{r}(\mu_j^2 - 1)\frac{d}{dr}w_j(r) \Big) + \mu_j M_{rr_j}(r).$$

$$(21)$$

Here it should be noticed that the stress resultants in the circumferential direction are expressed in terms of displacements, temperatures and stress resultants in the radial direction for brevity. In addition, it is seen that the stress resultants do not depend on the circumferential displacement.

Hence, through substitution of (21) into the field equations (19), and using the r dependent variables in the compatibility equations (18), the governing equations for face sheets ($j = t, b$) in the axisymmetric sandwich plate case read:

$$\mathbb{A}_j \Big(\frac{1}{2}(\mu_j + 1)r \frac{d}{dr}\big(T_{jt}(r) + T_{jb}(r)\big)\alpha_j + \frac{\mu_j - 1}{2}\Big(\frac{d}{dr}w_j(r)\Big)^2$$
$$- r\frac{d^2}{dr^2}u_{0j}(r) - r\frac{d}{dr}w_j(r)\frac{d^2}{dr^2}w_j(r) + \frac{1}{r}u_{0j}(r) - \frac{d}{dr}u_{0j}(r) \Big) + (-1)^k r\tau_r(r) - rn_{rr_j}(r) = 0,$$

$$\frac{1}{2}\mathbb{A}_j(\mu_j - 1)\frac{1}{r^2}\Big(r^3 \frac{d^2}{dr^2}v_{0j}(r) - v_{0j}(r) + r\frac{d}{dr}v_{0j}(r) \Big) + (-1)^k r\tau_\theta(r) - rn_{\theta\theta_j}(r) = 0,$$

$$-\frac{\alpha_j}{d_j}\mathbb{D}_j(1+\mu_j)\Big(r\frac{d^2}{dr^2}\big(T_{jb}(r)-T_{jt}(r)\big)+\frac{d}{dr}\big(T_{jb}(r)-T_{jt}(r)\big)\Big)-\frac{1}{2}\mathbb{A}_j\mu_j\Big(\frac{d}{dr}w_j(r)\Big)^3$$

$$+\mathbb{D}_j\Big(r\frac{d^4}{dr^4}w_j(r)+2\frac{d^3}{dr^3}w_j(r)-\frac{1}{r}\frac{d^2}{dr^2}w_j(r)+\frac{1}{r^2}\frac{d}{dr}w_j(r)\Big)+(-1)^k r\sigma_{zzj}(r)-rq_j(r)$$

$$+\Big(\Big(\frac{\mu_j+1}{2}\big(T_{jt}(r)+T_{jb}(r)\big)\alpha_j-\frac{u_{0j}(r)}{r}-\mu_j\frac{d}{dr}u_{0j}(r)\Big)\mathbb{A}_j+r\tau_r(r)+rn_{rr_j}(r)\Big)\frac{d}{dr}w_j(r)$$

$$-\mathbb{A}_j\Big(\frac{r}{2}\Big(\frac{d}{dr}w_j(r)\Big)^2+r\frac{d}{dr}u_{0j}(r)+u_{0j}(r)\mu_j-\frac{r}{2}\alpha_j(1+\mu_j)\big(T_{jt}(r)+T_{jb}(r)\big)\Big)\frac{d^2}{dr^2}w_j(r)$$

$$+r\frac{d}{dr}m_{rr_j}(r)+m_{rr_j}(r)-\frac{d_j}{2}\Big(\tau_r(r)+r\frac{d}{dr}\tau_r(r)\Big)=0. \quad (22)$$

And the compatibility equations equal:

$$-\frac{1}{12}c^2\frac{d}{dr}\big(T_{ct}(r)-T_{cb}(r)\big)\alpha_c-\frac{1}{2}(c+d_b)\frac{d}{dr}w_b(r)-\frac{1}{2}(c+d_t)\frac{d}{dr}w_t(r)-u_{0b}(r)+u_{0t}(r)$$

$$+\Big(\frac{c}{G_{rzc}}+\frac{1}{12}\frac{c^3}{E_{zc}r^2}\Big)\tau_{rz}(r)-\frac{c^3}{12E_{zc}r}\Big(\frac{d}{dr}\tau_{rz}(r)+r\frac{d^2}{dr^2}\tau_{rz}(r)\Big)=0,$$

$$\frac{\tau_\theta(r)c}{G_{\theta zc}}+v_{0t}(r)-v_{0b}(r)=0. \quad (23)$$

The interfacial vertical normal stresses read ($j=t,b$):

$$\sigma_{zzj}(r)=-\frac{E_{zc}}{2}\big(T_{cb}(r)+T_{ct}(r)\big)\alpha_c+\frac{E_{zc}}{c}\big(w_b(r)-w_t(r)\big)+\frac{1}{2r}(c-2z_{cj})\Big(r\frac{d}{dr}\tau_{rz}(r)+\tau_{rz}(r)\Big), \quad (24)$$

where $z_{cj}=0, c$ at the upper and the lower interfaces, respectively. The stress and displacements fields of the radially symmetric case can be determined by imposing the constraints that all dependent quantities are only dependent of the radial coordinate r; see (14) and (15).

In addition, when no in-plane external circumferential loads are imposed — see the second equation in (19) — and substituting this result into the second compatibility in (23), the following conditions are obtained:

$$\tau_\theta(r)=0, \quad v_{0t}(r)-v_{0b}(r)=0. \quad (25)$$

The physical interpretation of (25) is that the circumferential displacements in the upper and the lower face sheets must be identical and equal to zero, since no external displacements are imposed in this direction.

It should be noticed that for the case when the mechanical core properties are temperature-dependent, the solution procedure to determine the stress and displacements field of the core follows the approach outlined in [Frostig and Thomsen 2007; 2009], to which reference is made for brevity.

The nonlinear governing equations for the radially symmetric circular sandwich plate case can be expressed by a set of fourteen order ordinary differential equations (ODEs). The boundary value problem constituted by the set of ODEs together with the associated boundary condition can be solved using numerical schemes such as the multiple-point shooting method [Stoer and Bulirsch 1980], or the finite-difference (FD) approach using trapezoid or mid-point methods with Richardson extrapolation or deferred corrections [Ascher and Petzold 1998], as implemented in Maple, along with parametric or arc-length continuation methods [Keller 1992]. Here, the FD approach implemented in Maple has been used. In

the next section the results of a numerical study that discusses the thermomechanical nonlinear response of a radially symmetric sandwich plate are presented.

6. Numerical study

The nonlinear thermomechanical response of a radially symmetric circular sandwich plate with a foam core that has temperature-dependent mechanical properties loaded by a partially uniformly distributed load at mid-span is studied. First, the combined response of a uniformly heated plate with the partially distributed load is discussed with results along the plate and equilibrium curves. The equilibrium curves of temperature versus extreme values of displacements are compared with results of nonlinear finite element analyses (FEA) conducted using ABAQUS/Standard. This is followed by a study that includes the equilibrium curves where a temperature gradient is imposed across the sandwich plate thickness such that the temperature of the lower face sheets is higher than the temperature of the upper face sheet.

The specific sandwich plate configuration (see Figure 2a) consists of a circular sandwich plate with a diameter of 300 mm; two face sheets of 0.5 mm thickness with a coefficient of thermal expansion $\alpha_j = 0.00001$ ($j = t, b$) and made as glass/epoxy composite laminates, and a Divinycell HD-60 foam core with $E_{c0} = 52.5$ MPa and $G_{c0} = 20.2$ MPa (at 20°C) with a thickness of 19.05 mm with $\alpha_c = 0.00035$ made by DIAB [2003]. The supporting system imposed at the edge of the sandwich plate consists of a
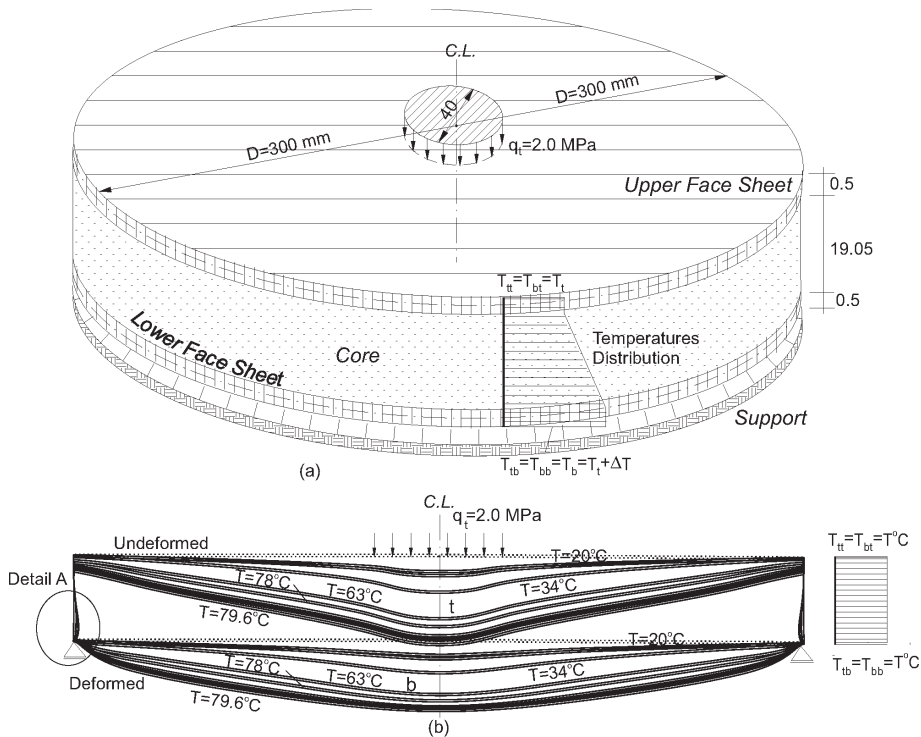
Figure 2. Circular sandwich plate geometry and deformed shapes: (a) plate layout, mechanical and thermal loads and supporting scheme; (b) deformed shape due to mechanical and uniformly distributed load.

horizontally moveable simple supports of the lower face sheet, while the upper face sheet and the core
are free of any displacement constrains or stress tractions. In addition, the center of the sandwich plate
is assumed to be horizontally immoveable. The loads system includes mechanical loads and an imposed
thermal field; see Figure 2a. The mechanical load consists of a patch load of uniform distribution of
2.0 MPa imposed at a circular area around center of plate with a diameter 40 mm at the upper face sheet,
and a temperature field with a linear through-thickness distribution in the core and uniform temperatures
through the thickness of the face sheets. The thermal gradient, ΔT, raises the temperature imposed on
the lower face sheet; see Figure 2a.

The temperature-dependent (TD) core properties are specified according to the Divinycell HD grade
PVC foam core data sheet [DIAB 2003], which includes measured material properties in a working range
of temperatures between 20 to 80°C. The mechanical properties of Divinycell PVC foam degrades as the
temperatures are raised and they are defined here through curve-fitting of the data that appears in [DIAB
2003] (see Figure 3a) as follows:

$$
\begin{aligned}
E_{zc}(r, z_c) &= E_{c0} f(T), \\
G_{rzc}(r, z_c) &= G_{c0} f(T), \\
f(T) &= -2.821963496 \ 10^{-13} \ T^8 + 9.528319971 \ 10^{-11} \ T^7 + 0.03070734934 \ T \\
&\quad - 1.325134998 \ 10^{-8} \ T^6 - 0.009541812399 \ T^2 + 9.703157671 \ 10^{-7} \ T^5 \\
&\quad + 0.0008705288588 \ T^3 - 0.00003952259514 \ T^4 + 1.1903,
\end{aligned}
\tag{26}
$$

where E_{c0} and G_{c0} refer to the elasticity and shear moduli of the core at $T = 20$°C. Notice that when
a thermal gradient is applied to the sandwich plate the mechanical properties of the core are dependent
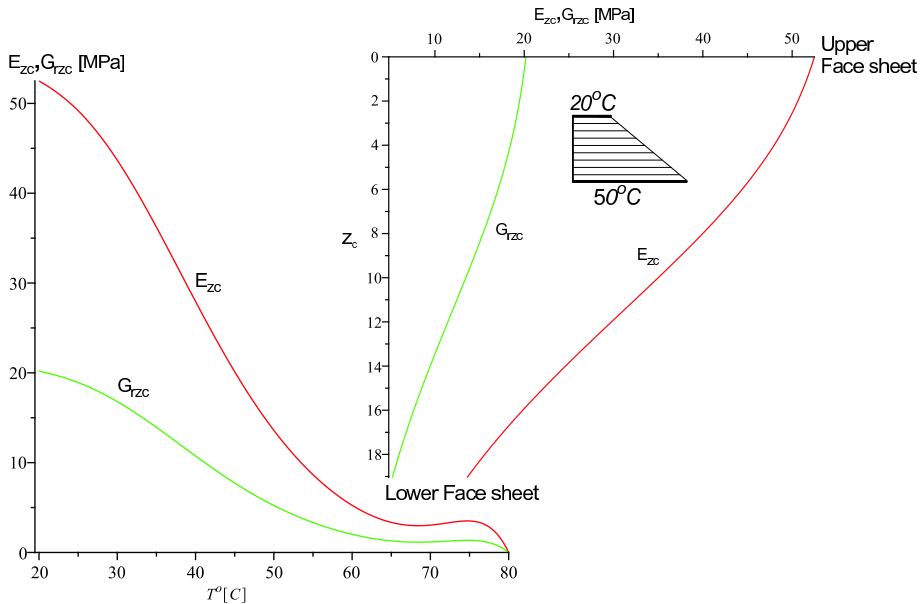
Figure 3. Elastic core moduli: (a) moduli magnitude versus temperatures; (b) moduli
distribution through depth of core.

on the vertical coordinate (Figure 3b). In addition, it is assumed here that the temperature dependence is identical for the modulus of elasticity and the shear modulus of the core. For further details see [Frostig and Thomsen 2007; 2009].

The solution procedure uses a parametric continuation method with the temperature T as the parameter. The procedure halts when the solution does not converge or when it violates the assumption of large displacements and moderate rotations (displacements exceeding D/10). The results are also limited to a temperature of 79.7°C, which is closed to the upper limit of the range of operating temperatures for the HD-60 foam considered; see DIAB [2003].

The first case presents the thermomechanical response of a circular sandwich plate with a uniformly distributed temperature through the plate thickness that changes from 20°C to 79.6°C, and a mechanical distributed load of 2.0 MPa partially distributed at center of plate; see Figure 2 for details. The deformed shapes at different temperature levels appear in Figure 2b from which it is observed that the deformation patterns display a significant indentation zone at the upper face sheet and a much smaller at the lower one. Or in other words the indentation deformation decays through the core thickness. It should be noticed that although the mechanical load has not been changed the indentation deepens and narrows as the temperature is raised as a result of the degradation of the temperature-dependent mechanical properties of the core. Moreover, localized in-plane displacements are observed in the core above the lower supports; see Detail A in Figure 2b. In addition, the radial in-plane displacements of the upper and the lower face sheets at the edges of the sandwich plate are very small as a result of the 2D in-plane action of the plate in the radial and circumferential directions although both edges are free to slide horizontally.

The predicted variations of selected structural quantities along the radius of the sandwich plate appear in Figure 4 for different temperatures. The vertical displacements of the face sheets (see Figure 4a) display an indentation at mid-span ($r = 0$) that deepens and narrows as the temperature is raised. It should be noticed that the displacements increase monotonically up to 78°C, after which disproportional increases of the displacements are observed as a result of the development of a limit point; see Figure 5a. In addition, the vertical displacements at the edge of the upper face sheet are not zero, due to the vertical flexibility of the core. The radial variation of the radial and the circumferential bending moment resultants for each face sheet (see Figure 4b) are associated with large values at the edges of the loaded area, around center of plate at the upper face sheet, and even larger in the vicinity of the edge of the lower face sheet due to the presence of the supports at this location. The in-plane face sheet stress resultants in the radial and circumferential directions are associated with tensile values around center, compressive values in the circumferential direction, and zero radial stress resultants at the edge of the sandwich plate; see Figure 4c. Please notice that at low temperatures, both stress resultants are in compression but the radial stress resultants change into tensile values as the temperature is raised, while the circumferential stress resultants change from tensile at center to compression at the plate edge. The radial in-plane mid-height displacements of the face sheets (see Figure 4d) are quite small in comparison with the vertical ones (see Figure 4a) but they reach large values at the face sheet edges at high temperatures. The radial interfacial shear stresses at the face-core interfaces are associated with large values in the vicinity of the edge of the loaded area and much smaller values toward the sandwich plate edge; see Figure 4e. Large interfacial vertical normal stresses are observed within the radial distance of the loaded area, at lower temperatures, as well as at the edge of the plate at high temperatures; see Figure 4f. At lower temperature levels the shear stresses in the core and the interfacial vertical normal stresses at the upper face sheet
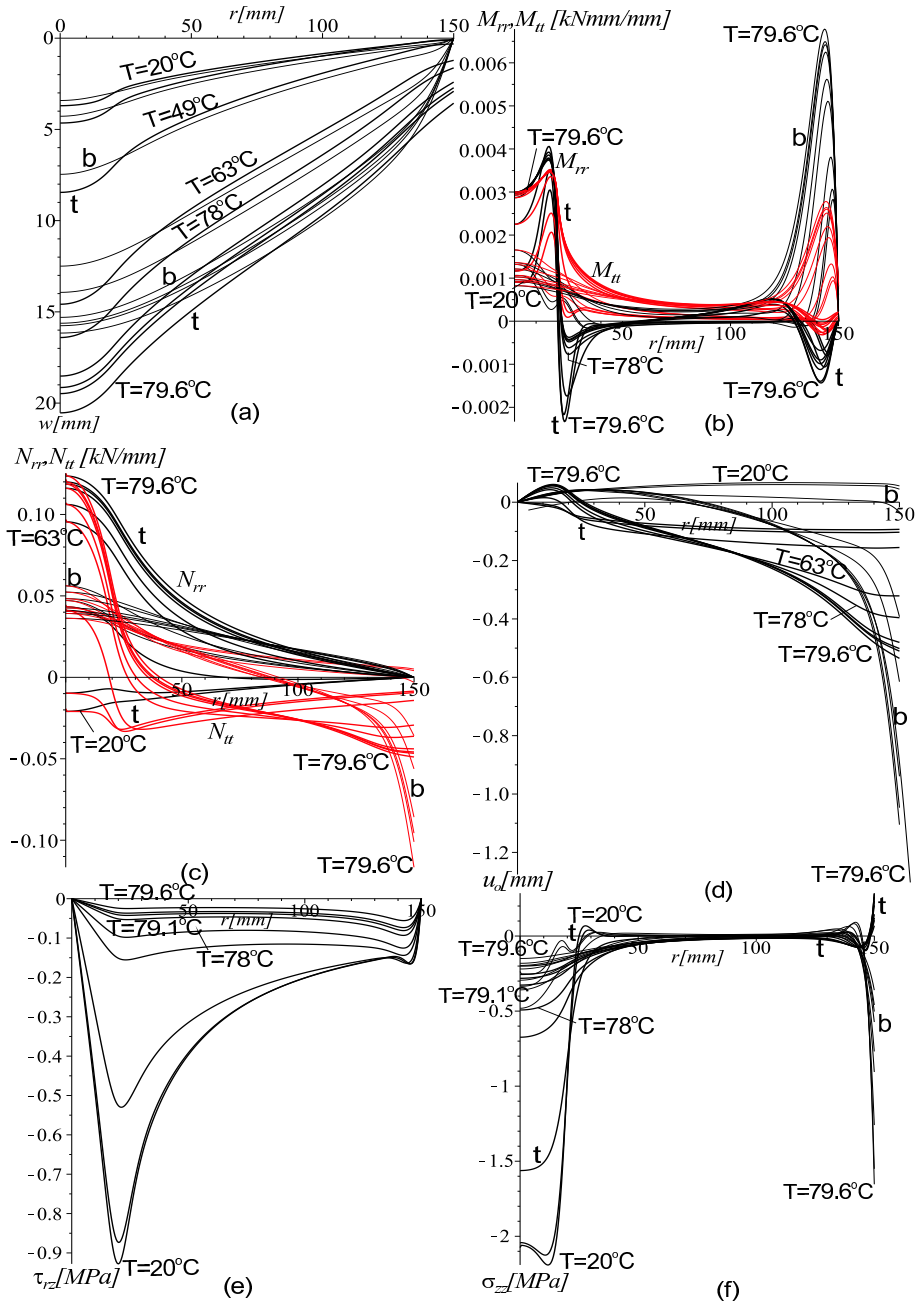
Figure 4. Thermomechanical radial response for a partially distributed load and a uniform temperature distribution. Face sheets: (a) vertical displacements; (b) radial and circumferential bending moments; (c) radial and circumferential in-plane stress resultants; (d) radial in-plane mid-height displacements. Core: (e) shear stresses; (f) face-core interfaces vertical normal stresses. Thicker black lines represent the upper face and thinner ones the lower face; red lines in (b) and (c) represent circumferential magnitudes.
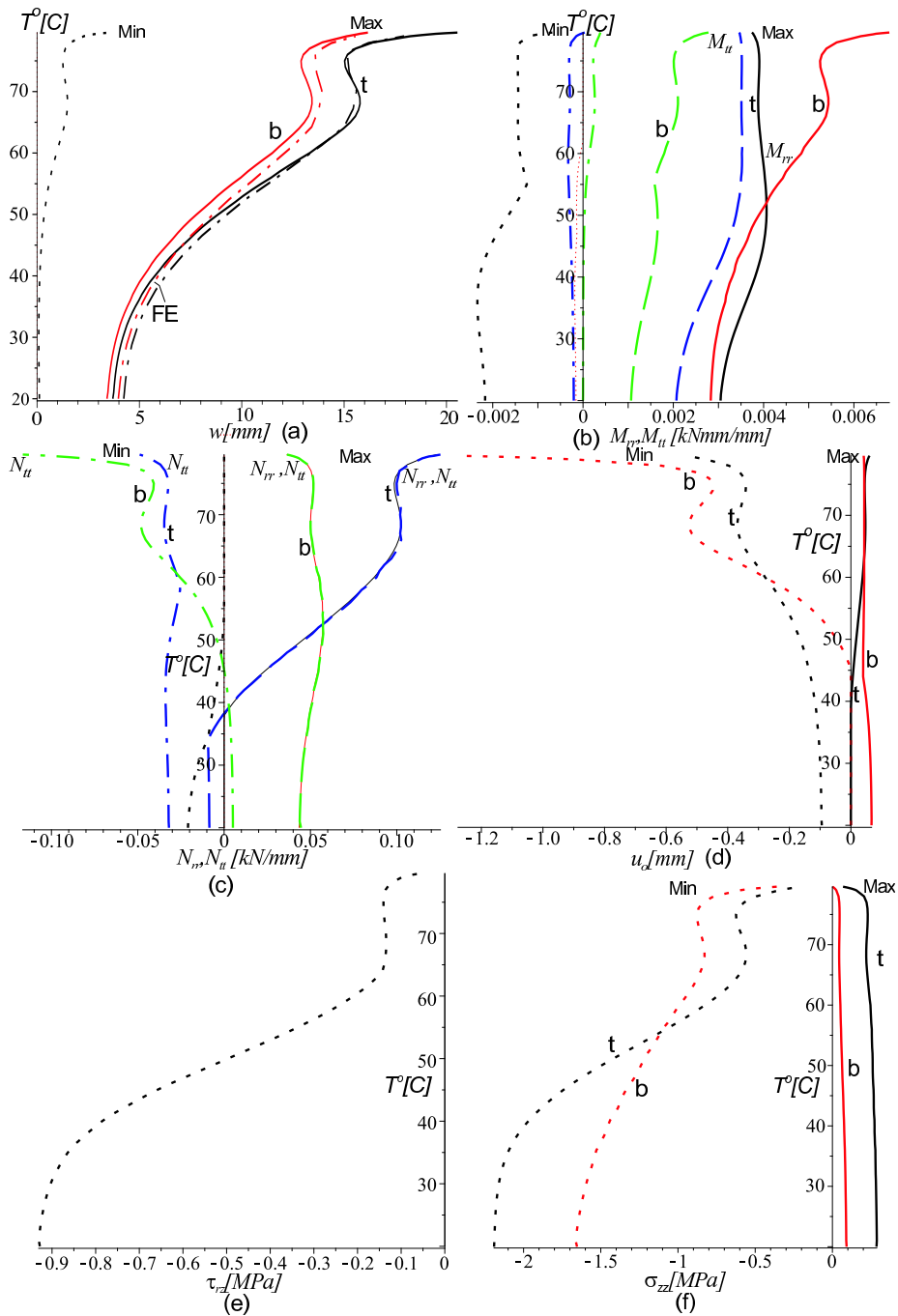
Figure 5. Equilibrium curves of temperature vs. extremum values of selected structural quantities for a partially distributed load and a uniform temperature distribution. Face sheets: (a) vertical displacements; (b) radial and circumferential bending moments; (c) radial and circumferential in-plane stress resultants; (d) radial in-plane mid-height displacements. Core: (e) shear stresses; (f) face-core interface vertical normal stresses.

are almost equal in magnitude to the applied pressure load, and they reduce as the temperature level increases. Actually, what happens is that as the mechanical properties of the degrade it stops carrying any more stresses and each face sheets behave as an independent plate rather than a part of the sandwich panel with a composite action that forms the couple in the face sheets. At the edge of the sandwich plate the interfacial vertical normal stresses change to tension at the upper interface and to compression at the lower interface due to the presence of the edge support system at the lower face sheet and the vertical displacements at the upper face, but without significant effects of the degradation of the mechanical core properties.

The equilibrium curves corresponding to the thermomechanical response are described by temperature versus extremum values of selected structural quantities; see Figure 5. The predicted curves of the extremum vertical displacements of the upper and the lower face sheets predicted by the nonlinear HSAPT model and the nonlinear FEA predictions using ABAQUS/Standard appear in Figure 5a. For details on the FEA modeling such as element types, material properties of the face sheets and material model for the core see [Santiuste et al. 2011]. Figure 5a reveals that loss of stability in the form of a limit point occurs as the temperatures are raised and the mechanical properties degrade. The FEA results compare very well with the HSAPT model, although the FEA results predict a slightly stiffer structure at almost all values of temperatures as expected. Similar trends are observed for the radial and circumferential bending moment resultant curves; see Figure 5b. Here it should be noticed that the largest bending moment resultants occur at the lower face sheet in the vicinity of the support (see also Figure 4b). The in-plane stress resultants in the radial and circumferential directions reveal a loss of stability at high temperatures. In addition, the circumferential stress resultants reach larger values in compression and tension as the temperatures are raised. The radial in-plane mid-height displacements of the face sheets (see Figure 5d) are associated with large values as the temperature is increased and approach the upper temperature range. The shear stresses in the core follow a different trend; see Figure 5e. At low temperatures the interfacial shear stresses are quite large and they decrease as the temperature is raised. The implication of this is that the contribution of the couple that forms in the sandwich plate (known also as the composite action) as a result of the overall bending is significantly reduced as the temperature is raised. The interfacial vertical normal stresses follow a similar trend as the interfacial shear stresses; see Figure 5f. Notice that at low temperatures the extremum compressive stresses at the upper interface are quite large and that they reduce as the temperature increases. The extremum tensile interfacial stresses are almost constant through the entire range of temperatures at the upper and the lower face sheets, and they almost disappear at high levels of temperature.

The effect of a temperature gradient between the upper and the lower face sheets, where the upper face sheet is at a temperature of T, whereas the lower face sheet is at a temperature of $T + \Delta T$. The maximum core temperature is increased to 79°C at the lower face sheet or to a temperature level where solution convergence is not achievable. Notice that under such conditions the moduli of the core are coordinate-dependent (varies in both radial and though-thickness directions) which require a special solution procedure that yields a closed-form solution for the core fields. For details see [Frostig and Thomsen 2007; 2009].

The equilibrium curves of temperature at the upper face-sheet versus extremum values of selected structural quantities for different temperature gradients appear in Figure 6. They consist of the results obtained for the temperature-dependent core (TD) using the moduli of the core that appear in Figure 3
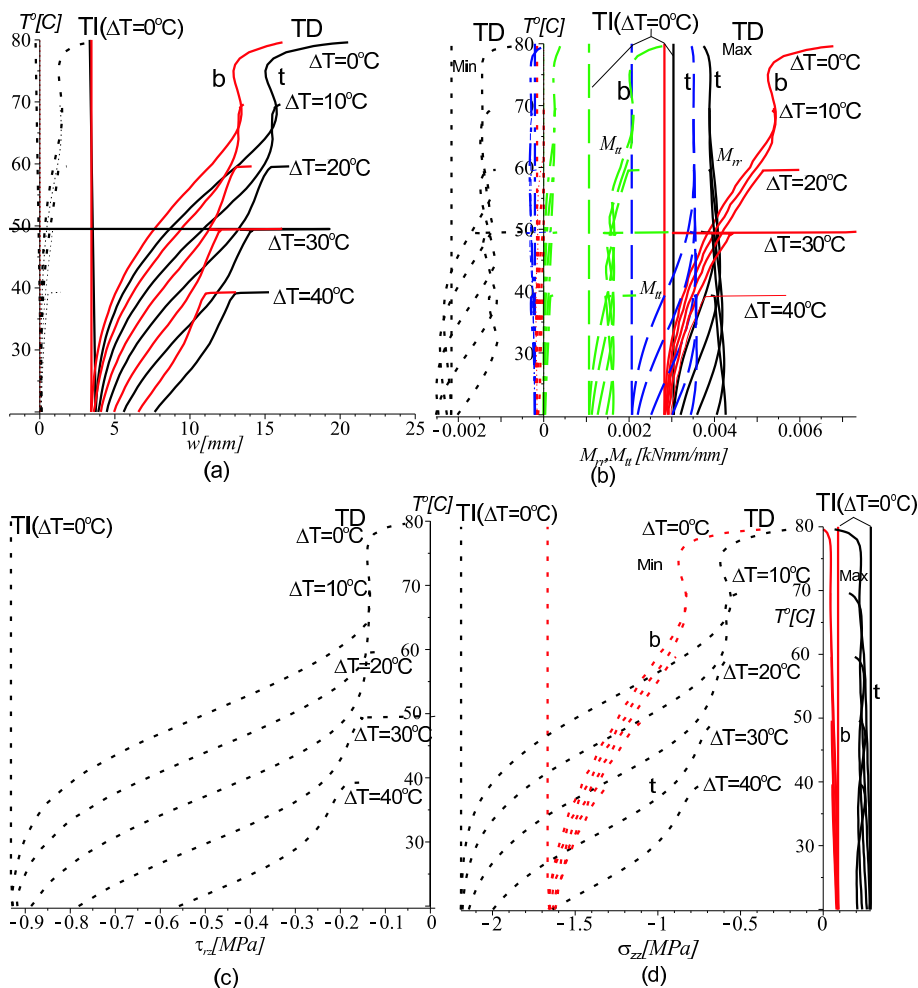
Figure 6. Equilibrium curves of temperature vs. extremum values of selected structural quantities for a partially distributed load and different thermal through-thickness gradients. Face sheets: (a) vertical displacements (HSAPT and FE); (b) radial and circumferential bending moments. Core: (c) shear stresses; (d) face-core interfaces vertical normal stresses.

and the case of a core with temperature-independent (TI) with moduli values that correspond to $T = 20°C$ and a zero thermal gradient. The plots of temperature versus the extreme vertical displacements appear in Figure 6a, and it is seen that at all thermal gradient levels a loss of stability is observed. It occurs when the temperature at the lower face sheet approaches the higher levels of the operating temperature of the core. Please notice that the degradation of core properties at the higher temperature is significant only within a small fraction of the core height near the lower face-core interface. The TI case exhibit linear behavior and is unaffected by the temperature level.

Similar trends are observed for the radial bending moment resultants (see Figure 6b) while the circumferential bending moment resultants are almost independent of the temperature.

The core shear stresses (see Figure 6c) follow an opposite trend; as the temperature is raised the core shear stresses decreases independent of the thermal gradient values. The vertical normal interfacial stresses follow the trends of the shear stresses; see Figure 6d. Notice that as the temperature is raised the vertical normal interfacial stress values decrease. In all cases the TI core exhibit linear results that are independent of the temperature levels and they are completely different than the results obtained when the thermal degradation of the foam core is taken into account.

7. Summary and conclusions

A general and rigorous systematic geometrically nonlinear high-order computational model of circular sandwich plates with general layout and a compliant core material is presented. The mathematical formulations outlines the derivation of the nonlinear field equations; the appropriate boundary conditions; as well as the stress and deformations fields of the core, when the sandwich plate is subjected to mechanical loads in parallel with thermally induced deformations and when the core properties are temperature-independent. The case of a sandwich core with temperature-dependent properties is also treated following the procedure outlined in [Frostig and Thomsen 2007; 2009]. In succession of this the special case of radially symmetric sandwich plates are considered and it yields the nonlinear governing equations for such plates when subjected to combined mechanical and thermal loads.

The results of a numerical study are presented. This includes the nonlinear load response characteristics of radially symmetric circular plates subjected to combined thermal and mechanical loads, as well as the effects of different thermal gradient values through the depth of the core.

The response is also associated with stress concentration regions due to localized effects such as at the edge of the loaded region as well as the support region. The shear and interfacial vertical normal stresses results reveal that as the temperatures are raised the collaboration between the face sheets diminishes and the load transfer mechanism is associated with independent significant bending in each face sheet rather than as part of a composite action that form a couple in an ordinary sandwich panels. Loss of stability is observed as the temperatures approach the upper limit of the range of working temperature. In general, it is associated with very large displacements, bending moments and in-plane stress resultants.

The conducted numerical study reveals that the response becomes unstable as the temperature is increased and the mechanical core properties degrade. Hence, in such cases the design of sandwich structures should be controlled by stability criteria rather than stress constraints.

The effects of imposing different thermal gradients across the core thickness have also been examined. Notice that when the temperature distribution through the core depth is not uniform the core stiffness parameters will vary through the core thickness. This requires a special solution procedure. It has been found that for temperature gradient levels a loss of stability occurs when the temperature at the tensile face sheet approaches the upper limit of the temperature range.

In general, the nonlinear response of a circular sandwich plate is much stiffer than the case of a unidirectional sandwich panel or beam. When comparing with the sandwich panel or beam cases, the presence of circumferential rigidity in addition to the longitudinal rigidity improves the stiffness of the sandwich circular plate. Thus, the presence of a 2D in-plane stress field stabilizes the load response of sandwich plates when compared to the unidirectional panel/beam response characteristics. However, the use of core materials with temperature-dependent mechanical properties that degrade with increasing

temperature yields an unstable response independent of the structural configuration (1D beam/panel or 2D plate). Hence, a reliable design of any type of sandwich structure must take into account the loss of stability that may occur within the working range of temperatures due to thermal degradation when compliant sandwich core materials are used.

Acknowledgments

References

[Allen 1969] H. G. Allen, *Analysis and design of structural sandwich panels*, Pergamon, Oxford, 1969.

[Ascher and Petzold 1998] U. M. Ascher and L. R. Petzold, *Computer methods for ordinary differential equations and differential-algebraic equations*, SIAM, Philadelphia, 1998.

[DIAB 2003] *Data sheet for Divinycell HD grade PVC foams*, DIAB, Laholm, 2003.

[Du 1994] G. Du, "Large amplitude vibration of circular sandwich plates", *Appl. Math. Mech.* **15**:5 (1994), 461–469.

[Du and Li 2000] G. Du and H. Li, "Nonlinear vibration of circular sandwich plate under the uniformed load", *Appl. Math. Mech.* **21**:2 (2000), 217–226.

[Frostig and Thomsen 2007] Y. Frostig and O. T. Thomsen, "Buckling and nonlinear response of sandwich panels with a compliant core and temperature-dependent mechanical properties", *J. Mech. Mater. Struct.* **2**:7 (2007), 1355–1380.

[Frostig and Thomsen 2009] Y. Frostig and O. T. Thomsen, "Nonlinear behavior of thermally loaded curved sandwich panels with a transversely flexible core", *J. Mech. Mater. Struct.* **4**:7–8 (2009), 1287–1326.

[Frostig et al. 1992] Y. Frostig, M. Baruch, O. Vilnay, and I. Sheinman, "High-order theory for sandwich-beam behavior with transversely flexible core", *J. Eng. Mech.* (*ASCE*) **118**:5 (1992), 1026–1043.

[Gupta and Jain 1982] A. P. Gupta and M. Jain, "Axisymmetric vibrations of annular sandwich plates of linearly varying thickness", *J. Sound Vib.* **80**:3 (1982), 329–337.

[Gupta and Sharma 1982] A. P. Gupta and K. P. Sharma, "Axisymmetric flexure of circular sandwich plate including transverse shear in facings", *Z. Angew. Math. Mech.* **62**:10 (1982), 533–538.

[Hohe and Librescu 2004] J. Hohe and L. Librescu, "Advances in the structural modeling of elastic sandwich panels", *Mech. Adv. Mater. Struct.* **11**:4–5 (2004), 395–424.

[Kao 1970] J.-S. Kao, "Bending of circular sandwich plates due to asymmetric temperature distribution", *AIAA J.* **8**:5 (1970), 951–954.

[Keller 1992] H. B. Keller, *Numerical methods for two-point boundary value problems*, Dover, New York, 1992.

[Librescu and Hause 2000] L. Librescu and T. Hause, "Recent developments in the modeling and behavior of advanced sandwich constructions: a survey", *Compos. Struct.* **48**:1–3 (2000), 1–17.

[Mindlin 1951] R. D. Mindlin, "Influence of transverse shear deformation on the bending of classical plates", *J. Appl. Mech.* (*ASME*) **8** (1951), 18–31.

[Montrey 1973] H. M. Montrey, "Bending of a circular sandwich plate by load applied through an insert", Research paper FPL 201, Forest Products Laboratory, Forest Service, United States Department of Agriculture, Madison, WI, 1973, Available at http://www.fpl.fs.fed.us/documnts/fplrp/fplrp201.pdf.

[Noor et al. 1996] A. K. Noor, W. S. Burton, and C. W. Bert, "Computational models for sandwich panels and shells", *Appl. Mech. Rev.* (*ASME*) **49**:3 (1996), 155–199.

[Petras and Sutcliffe 2000] A. Petras and M. P. F. Sutcliffe, "Indentation failure analysis of sandwich beams", *Compos. Struct.* **50**:3 (2000), 311–318.

[Plantema 1966] F. J. Plantema, *Sandwich construction*, Wiley, New York, 1966.

[Rabinovitch and Frostig 2002a] O. Rabinovitch and Y. Frostig, "High-order behavior of fully bonded and delaminated circular sandwich plates with laminated face sheets and a "soft" core", *Int. J. Solids Struct.* **39**:11 (2002), 3057–3077.

[Rabinovitch and Frostig 2002b] O. Rabinovitch and Y. Frostig, "Strengthening of RC slabs with circular composite patches: a high-order approach", *Compos. Struct.* **55**:2 (2002), 225–238.

[Rabinovitch and Frostig 2004a] O. Rabinovitch and Y. Frostig, "High-order analysis of reinforced concrete slabs strengthened with circular composite laminated patches of general layup", *J. Eng. Mech.* (*ASCE*) **130**:11 (2004), 1334–1345.

[Rabinovitch and Frostig 2004b] O. Rabinovitch and Y. Frostig, "Delamination effects in reinforced concrete slabs strengthened with circular composite patches", *J. Eng. Mech.* (*ASCE*) **130**:12 (2004), 1436–1446.

[Reddy 1984] J. N. Reddy, *Energy and variational methods in applied mechanics*, Wiley, New York, 1984.

[Rohacell 2004] Evonik Degussa, *Rohacell: WF foam data sheets*, Rohacell, Essen, 2004, Available at http://www.rohacell.com.

[Santiuste et al. 2011] C. Santiuste, O. T. Thomsen, and Y. Frostig, "Thermo-mechanical load interactions in foam cored axi-symmetric sandwich circular plates: high-order and FE models", *Compos. Struct.* **93**:2 (2011), 369–376.

[Selke 1971] L. A. Selke, "Theoretical elastic deformations of solid and cored horizontal circular mirrors having a central hole on a ring support", *Appl. Opt.* **10**:4 (1971), 939–944.

[Sherif 1992] H. A. Sherif, "Free flexural vibrations of clamped circular sandwich plates", *J. Sound Vib.* **157**:3 (1992), 531–537.

[Stoer and Bulirsch 1980] J. Stoer and R. Bulirsch, *Introduction to numerical analysis*, Springer, New York, 1980.

[Thomsen 1995] O. T. Thomsen, "Theoretical and experimental investigation of local bending effects in sandwich plates", *Compos. Struct.* **30**:1 (1995), 85–101.

[Thomsen 1997] O. T. Thomsen, "Sandwich plates with 'through-the-thickness' and 'fully potted' inserts: evaluation of differences in structural performance", *Compos. Struct.* **40**:2 (1997), 159–174.

[Thomsen and Rits 1998] O. T. Thomsen and W. Rits, "Analysis and design of sandwich plates with inserts: a high-order sandwich plate theory approach", *Compos. B Eng.* **29**:6 (1998), 795–807.

[Vinson 1999] J. R. Vinson, *The behavior of sandwich structures of isotropic and composite materials*, Technomic, Lancaster, 1999.

[Wang 1995a] C. M. Wang, "Buckling of polygonal and circular sandwich plates", *AIAA J.* **33**:5 (1995), 962–964.

[Wang 1995b] C. M. Wang, "Deflection of sandwich plates in terms of corresponding Kirchhoff plate solutions", *Arch. Appl. Mech.* **65**:6 (1995), 408–414.

[Zenkert 1995] D. Zenkert, *An introduction to sandwich construction*, Chameleon, London, 1995.

[Zhou and Stronge 2006] D. Zhou and W. J. Stronge, "Modal frequencies of circular sandwich panels", *J. Sandw. Struct. Mater.* **8**:4 (2006), 343–357.

YEOSHUA FROSTIG: cvrfros@techunix.technion.ac.il
Professor, Ashtrom Engineering Company Chair in Civil Engineering
Technion - Israel Institute of Technology, Faculty of Civil and Environmental Engineering, Haifa, 32000, Israel

OLE THOMSEN: ott@me.aau.dk
Professor, Head of Department
Aalborg University, Department of Mechanical Engineering, Pontoppidanstræde 105, 9220 Aalborg Ø, Denmark

JOURNAL OF MECHANICS OF MATERIALS AND STRUCTURES

jomms.org

Founded by Charles R. Steele and Marie-Louise Steele

Cover design: Alex Scorpan   Cover photo: Ev Shafrir